Combining in Situ NEXAFS Spectroscopy and CO_2 Methanation Kinetics To Study Pt and Co Nanoparticle Catalysts Reveals Key Insights into the Role of Platinum in Promoted Cobalt Catalysis

Simon K. Beaumont,[†,‡,§,⊗] Selim Alayoglu,[†,‡,⊗] Colin Specht,[†,‡] William D. Michalak,[†,‡] Vladimir V. Pushkarev,[†,‡,×] Jinghua Guo,[∥,⊥] Norbert Kruse,[#,∇] and Gabor A. Somorjai*,[†,‡]

[†]Department of Chemistry, University of California, Berkeley, California 94720, United States

[‡]Materials Sciences Division and [∥]Advanced Light Source, Lawrence Berkeley National Laboratory, Berkeley, California 94720, United States

[§]Department of Chemistry, Durham University, South Road, Durham DH1 3LE, United Kingdom

[⊥]Department of Chemistry and Biochemistry, University of California, Santa Cruz, California 95064, United States

[#]Chimie Physique des Matériaux, Université Libre de Bruxelles, Campus de la Plaine CP 243, B-1050 Bruxelles, Belgium

[∇]Department of Chemical Engineering and Bioengineering, Washington State University, Pullman, Washington 99164, United States

Ⓢ Supporting Information

ABSTRACT: The mechanistic role of platinum and precious metals in promoting cobalt hydrogenation catalysts of the type used in reactions such as Fischer–Tropsch synthesis is highly debated. Here we use well-defined monometallic Pt and Co nanoparticles (NPs) and CO_2 methanation as a probe reaction to show that Pt NPs deposited near Co NPs can enhance the CO_2 methanation rate by up to a factor of 6 per Co surface atom. In situ NEXAFS spectroscopy of these same Pt NP plus Co NP systems in hydrogen shows that the presence of nearby Pt NPs is able to significantly enhance reduction of the Co at temperatures relevant to Fischer–Tropsch synthesis and CO_2 methanation. The mechanistic role of Pt in these reactions is discussed in light of these findings.

Platinum and other precious metals are known to promote cobalt catalysts for the reaction of CO and H_2 to hydrocarbons, known as Fischer–Tropsch synthesis. This reaction, initially developed by Franz Fischer and Hans Tropsch to the point of practical use in the early 20th century, is considered to be a viable option to partially replace crude oil derived transportation fuels, and therefore of considerable current interest.[1,2] Industrial Fischer–Tropsch synthesis now produces >200,000 barrels per day of synthetic oil.[1] Such catalysts have also been identified to be attractive as possible catalysts for CO_2 hydrogenation,[3,4] an analogous reaction that is desirable as a means of utilizing the greenhouse gas CO_2 to generate useful products. The latter is useful both for offsetting the cost of CO_2 capture and removing the need for subsequent CO_2 storage in CO_2 emission reduction schemes.[5] In either case, the role of Pt in promoting Co-catalyzed reactions of this type is generally not well understood, with a number of alternative explanations being offered for Pt's role. These can be classified as both structural and chemical effects—the former changing the dispersion of the Co and the latter influencing the catalytic chemistry.[6] It has been postulated this could include

intimate contact between the two metals modifying the local band structure, ensemble-type geometric effects, prevention of deactivation by carbonaceous deposits, and improvement in the reducibility of Co.[7–11] Interestingly for the present work, in a series of papers on Pd–Co sol–gel catalysts for CO hydrogenation, palladium is postulated to produce hydrogen that both facilitates Co reduction and participates in the reaction.[12–14] Considerable attempts have also been made using aberration corrected scanning transmission electron microscopy to establish the possible role of precious metals in these reactions. In the impregnated commercial-type catalysts studied, Pt appeared as a surface atomic species within Co particles, but notably also improved the apparent reducibility of Co particles containing no precious metal atoms, suggesting hydrogen spillover was occurring.[15] Although PtCo phases have been seen by X-ray diffraction,[10] no isolated Pt particles have been observed in studies on commercial-type catalysts. Nevertheless, it is useful for understanding the role of Pt to investigate what happens when isolated Pt particles are used as the promoter.

Controlled nanomaterials synthesis affords a new way to address such problems and has been employed to good effect in answering other key questions in catalysis.[16] The use of nanomaterials to address questions specifically in the study of Co-based catalysts for Fischer–Tropsch synthesis has recently been reviewed,[17] and we have already used size controlled Co nanoparticles (NPs) to explore particle size effects in CO_2 hydrogenation.[18] To understand better the exact role of precious metals in these types of catalysts, we have recently reported on the preparation of Pt–Co bimetallic NPs, where each NP contains an approximately 1:1 atomic ratio of the two metals. However, we found that these particles were poor CO_2 methanation catalysts. We identified this was attributable to Pt segregating to the surface in reducing conditions as demonstrated by ambient pressure X-ray photoelectron spec-

troscopy and environmental transmission electron microscopy in H_2.[3]

Here, we identify a different, more realistic model for the catalyst structure involved in the Pt promotional effect. Instead of the two metals being present within a single NP, we have instead taken discrete monometallic NPs of both Pt and Co and deposited them in close proximity within the pores of a mesoporous silica, MCF-17. This new structural model for the catalyst is a much better mimic for Pt promotion effects, exhibiting a methane production rate ~6 times that of pure Co NPs.

The various NPs can be deposited in both 3D (within the pores of a mesoporous silica, MCF-17) and 2D forms (on the native oxide surface of a silicon wafer). The 3D and 2D forms allow us to employ the same NPs for catalytic and X-ray spectroscopy measurements, respectively. Figure 1 shows
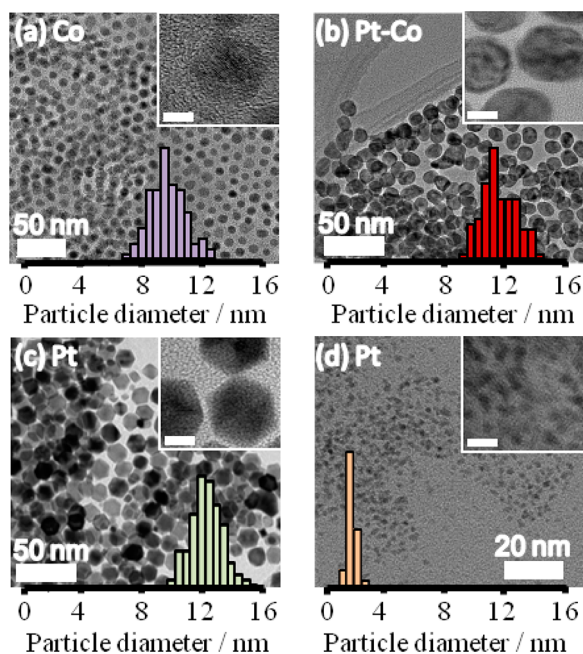
Figure 1. Transmission electron micrographs of as-prepared nanoparticles, overlaid with particle size distributions. Insets show HRTEM images for each system (5 nm scale bar): (a) 10 ± 1 nm Co NPs, (b) 11 ± 1.5 nm Pt−Co alloyed NPs (as previously reported), (c) 12 ± 1 nm Pt NPs, and (d) 1.9 ± 0.3 nm Pt NPs.

micrographs of all the NP samples used in this study: Co NPs and Co−Pt bimetallic NPs (as for our previous work on CO_2 hydrogenation), but additionally 12 and 1.9 nm Pt NP samples, with good size control as indicated by the overlaid particle size distributions. We mostly focus on the sample that results from combining 12 nm Pt and 10 nm Co, as this is closely matched in size to the pure Co and Co−Pt samples considered previously.

For the samples supported on MCF-17 used as catalysts in CO_2 hydrogenation, the turnover frequency (TOF) values for methane production at 200 °C are shown in Figure 2, along with a schematic representation of the compositions of the catalysts. 200 °C was deliberately chosen as the reaction temperature because of the typical range of commercial operating temperatures (200−250 °C) for the analogous CO hydrogenation or Fischer−Tropsch reaction. As previously reported and discussed above, pure Co NPs significantly
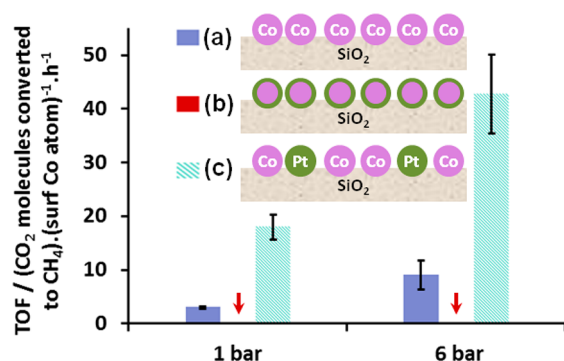

Figure 2. Turnover frequencies at 1 and 6 bar total pressure for the production of CH_4 during catalytic CO_2 hydrogenation (1:3 CO_2: H_2) at 200 °C for three catalyst samples: (a) 10 nm Co NPs supported on MCF-17 mesoporous silica, (b) 11 nm Co−Pt binary NPs supported on MCF-17, and (c) 10 nm Co and 12 nm Pt NPs mixed in solution and subsequently supported on MCF-17. The red arrows denote the position of the data points for the Co−Pt binary NP sample (indicating only trace amounts of CH_4). Schematic inset indicates overall structure of each sample.

outperform the Co−Pt bimetallic NPs, attributable to Pt segregating to the surface of each particle and inhibiting the reaction. However, pure Pt NPs located "near" the pure Co NPs (within the same mesoporous oxide support) result in a catalyst several times more active per Co site for the production of methane than their pure Co catalyst counterparts. It should be noted that this equates to around only 1 Pt NP for every 24 Co NPs (based on their average size and the loadings determined by ICP-AES, the latter indicating a Pt:Co molar ratio of ~1:20). This is slightly more than the often <1:100 molar ratio found in commercial-type catalysts to allow us to characterize the Pt NPs present with a range of techniques. We have previously demonstrated that the pure Pt NPs are inactive for this reaction;[3] therefore, we assume that all CH_4 production is derived from the pure Co particles. The dramatic increase in rate is therefore the result of Pt NPs enhancing the activity of the Co. Some production of CO is seen in all cases, along with very small traces of C_2 and higher hydrocarbon products.

One likely role for the Pt particles in this case is the efficient reduction of the Co particles' surfaces, as is often postulated for the role of precious metals in promoting Co catalysts for Fischer−Tropsch synthesis. Here, however, we pre-activated the Co catalyst by reduction at 450 °C in H_2, a treatment anticipated to afford fully reduced Co NPs; we have previously reported a water loss/hydrogen adsorption temperature-programmed reduction peak at this temperature for pure Co NP-based catalysts.[18]

Oxidation by water (a reaction product) is often considered to be a possible deactivation mechanism during Co-catalyzed hydrogenations,[19,20] although others have been unable to observe this during in situ near-edge X-ray absorption fine structure (NEXAFS) spectroscopy of Co crystallites in a 1:1 mix of H_2O and H_2.[21] However, if methane (or other hydrocarbon) formation occurs after breaking carbon−oxygen bonds in CO_2, oxygen may accumulate on (and beneath) the surface eventually leading to near surface oxidation before water is formed (Figure 3a). This will decrease the reaction rate, in agreement with findings on Co foils in vacuum for CO reduction, where hydrogenation and removal of surface oxide rather than the dissociation of CO were the rate limiting step.[22] It is also consistent with the recent observation using transient
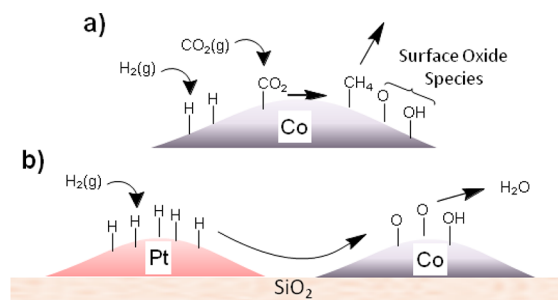
Figure 3. Schematics showing (a) production of surface oxide from CO/CO_2 hydrogenation and (b) transfer of adsorbed hydrogen from Pt to Co via a spillover mechanism to re-reduce the cobalt oxide surface, releasing water.

kinetic analysis for CO hydrogenation over a Co/MgO catalyst that oxygen (as well as carbon and hydrogen) builds up on the surface leading to more than a monolayer of adsorbed surface species under working conditions.[23]

Since Pt is very well known for dissociative chemisorption of H_2, we propose that hydrogen could be transferred between Pt and Co (as indicated in Figure 3b) to clean off surface oxygen/oxide under catalytic conditions. Such hydrogen transport processes theoretically involve the presence of surface hydroxyl groups, however it has been shown that silica surfaces typically have 6−7 OH groups per nm^2, even after 450 °C treatment in vacuum.[24] This hydrogen migration would reverse the deactivation, increasing the observed rate, as found during the catalytic experiments when Pt NPs are added. To investigate this further, we performed in situ NEXAFS spectroscopy during NP reduction for analogous 2D samples deposited on silicon wafers (Figure 4). Three samples were studied using NEXAFS: (1) pure Co NPs, (2) pure Co NPs with the same 12 nm Pt NPs (as used in the MCF-17 supported catalyst), and (3) pure Co NPs with smaller 1.9 nm Pt NPs (see Supporting Information (SI) for ex situ characterization). Samples were prepared by sequential dip-coating to yield films of individual Pt and Co NPs. This last sample with smaller Pt NPs was investigated to see whether the same effect would occur irrespective of Pt NP size (important in matching up to commercial catalysts, where only very small amounts of Pt are present[1]).

By comparing the sample spectra in Figure 4a−c with the reference spectra in Figure 4d, it is clear that a gradual change from the oxidized form toward a reduced Co metallic state occurs in all three samples as the temperature is increased. This can be seen especially clearly for the samples at 175 °C in Figure 4e. It can also be seen in Figure 5, which shows the fraction of metallic Co observed under each condition, obtained by using linear combinations of reference spectra to calculate the Co average valence, as is common for processing NEXAFS data of this kind.[25] At all temperatures investigated, it is clear that the fraction of Co reduced by H_2 to the metallic state is significantly higher when Pt NPs are added.

Since surface oxygen is more stable (imposes less lattice strain and decreases surface energy), it is reasonable to assume residual oxygen in the NP will preferentially diffuse to the surface on the time scale of our experiments, and therefore undergo reduction last. This means that the threshold for reducing a significant fraction of the surface Co atoms (marked in Figure 5) is achieved only in the presence of nearby Pt NPs, even at the upper temperature in the present study.
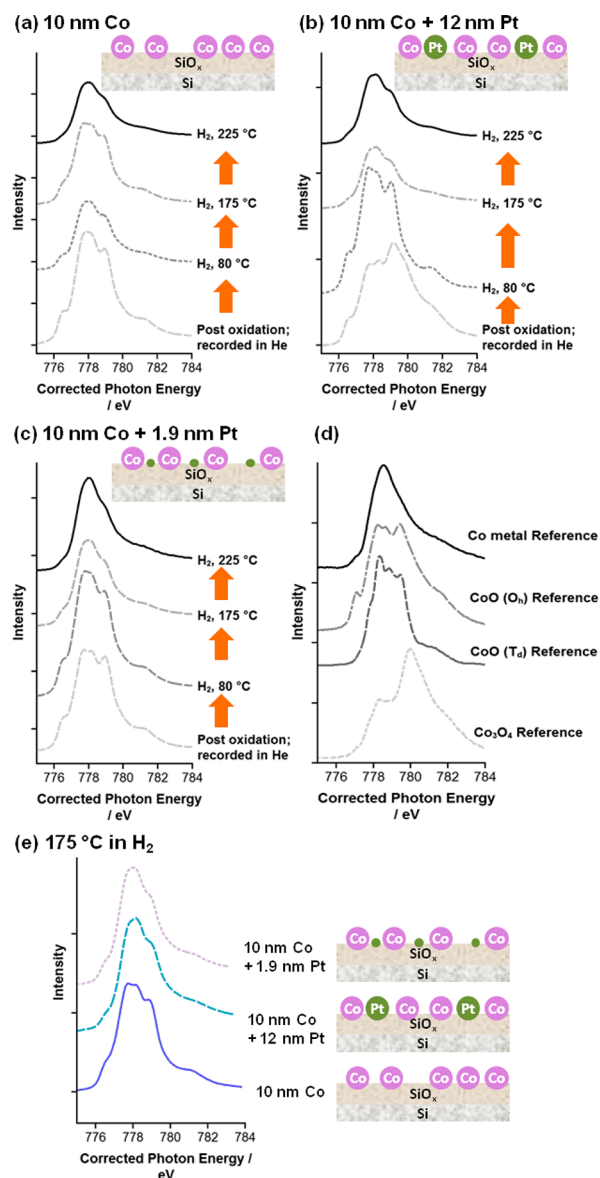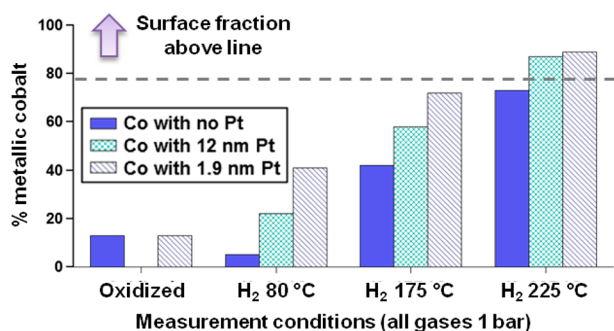

Figure 4. In situ Co L_3-edge NEXAFS spectra in H_2 at increasing temperatures, following oxidation in a He/O_2 mixture at 100 °C and cooling in He (a−c). A number of standard reference spectra obtained in vacuum are shown in (d), and the 175 °C spectra recorded in H_2 are replotted in (e) to facilitate comparison. Schematics indicate the overall structure of each sample.

As a final aside it is worth noting that we have, to date, been unsuccessful in preparing a uniform bimetallic NP sample (in the >6 nm range known to be active for CO and CO_2 hydrogenation) in which the Pt concentration is sufficiently low that Pt cannot cover most of the surface once segregated by the reducing atmosphere. When lower Pt concentration samples are targeted, a mixture of pure Co and Pt−Co NPs with higher Pt concentrations are produced. We therefore speculate that the surface reduction of Pt and Co salts during wet impregnation (the technique typically used to prepare commercial supported catalysts) is subject to similar constraints. The alternative role of Pt found here may be a very important feature of the promotional role precious metals have in industrially employed catalysts.

In summary, while bimetallic nanoparticles comprising Pt and Co within a single particle are ineffective as CO_2

Figure 5. Calculated % of metallic cobalt (Co^0) during in situ reduction. Data points based on least-squares fitting of the Co L_3-edge NEXAFS spectra to reference data shown in Figure 3d. The area above the horizontal line shows the fraction of the signal expected to originate from Co in the surface atomic layer; see SI. An example fitting and complete fitting results are also given in the SI.

hydrogenation catalysts, supporting individual Pt and Co NPs in close proximity on silica (even in a ~1:24 particle ratio) enhances the hydrogenation of CO_2 to CH_4 per Co surface atom over Co NPs by up to a factor of 6. In situ NEXAFS spectroscopy during Co NP reduction shows that the addition of Pt NPs is able to significantly enhance reduction of the Co at any given temperature. This allows us to tentatively suggest that hydrogen atoms dissociated on Pt may be transferred to the Co NPs via long-distance hydrogen atom spillover, aiding their reduction. Given the similar temperature range of the catalytic and spectroscopic results, the same phenomenon can be expected to occur under reaction conditions and therefore likely enhances the rate of removal of surface cobalt oxide formed in the reaction, generating more reaction sites and therefore rationalizing the observed dramatic increase in CH_4 production. Given the similar mechanisms, this observation also has implications for the role of Pt in promoting the analogous and industrially important Fischer−Tropsch (CO hydrogenation) reaction.

ASSOCIATED CONTENT

S Supporting Information

Methodology, NEXAFS spectra fitting, ex situ characterization of NEXAFS 2D and silica-supported Pt and Co 3D samples, surface fraction calculations, and ICP-AES. This material is available free of charge via the Internet at http://pubs.acs.org.

AUTHOR INFORMATION

Corresponding Author
somorjai@berkeley.edu

Present Address
×V.V.P.: Dow Corning Corp., Midland, MI 48686

Author Contributions
⊗S.K.B. and S.A. contributed equally.

Notes
The authors declare no competing financial interest.

ACKNOWLEDGMENTS

REFERENCES

(1) de Klerk, A. *Fischer−Tropsch Refining*; Wiley-VCH: Weinheim, 2012.

(2) Khodakov, A. Y.; Chu, W.; Fongarland, P. *Chem. Rev.* **2007**, *107*, 1692.

(3) Alayoglu, S.; Beaumont, S. K.; Zheng, F.; Pushkarev, V. V.; Zheng, H. M.; Iablokov, V.; Liu, Z.; Guo, J. H.; Kruse, N.; Somorjai, G. A. *Top. Catal.* **2011**, *54*, 778.

(4) Srisawad, N.; Chaitree, W.; Mekasuwandumrong, O.; Shotipruk, A.; Jongsomjit, B.; Panpranot, J. *React. Kinet., Mech. Catal.* **2012**, *107*, 179.

(5) D'Alessandro, D. M.; Smit, B.; Long, J. R. *Angew. Chem., Int. Ed.* **2010**, *49*, 6058.

(6) Iglesia, E. *Appl. Catal. A: General* **1997**, *161*, 59.

(7) Diehl, F.; Khodakov, A. Y. *Oil Gas Sci. Technol.—Rev. Inst. Fr. Pet.* **2009**, *64*, 11.

(8) Schanke, D.; Vada, S.; Blekkan, E. A.; Hilmen, A. M.; Hoff, A.; Holmen, A. *J. Catal.* **1995**, *156*, 85.

(9) Morales, F.; Weckhuysen, B. M. In *Catalysis*; Spivey, J. J., Dooley, K. M., Eds.; The Royal Society of Chemistry: Cambridge, 2006; Vol. 19.

(10) Dees, M. J.; Ponec, V. *J. Catal.* **1989**, *119*, 376.

(11) Batley, G. E.; Ekstrom, A.; Johnson, D. A. *J. Catal.* **1974**, *34*, 368.

(12) Guczi, L.; Borko, L.; Schay, Z.; Bazin, D.; Mizukami, F. *Catal. Today* **2001**, *65*, 51.

(13) Guczi, L.; Hoffer, T.; Zsoldos, Z.; Zyade, S.; Maire, G.; Garin, F. *J. Phys. Chem.* **1991**, *95*, 802.

(14) Guczi, L.; Schay, Z.; Stefler, G.; Mizukami, F. *J. Mol. Catal. A: Chem.* **1999**, *141*, 177.

(15) Shannon, M.; Lok, C.; Casci, J. *J. Catal.* **2007**, *249*, 41.

(16) Somorjai, G. A.; Contreras, A. M.; Montano, M.; Rioux, R. M. *Proc. Natl. Acad. Sci. U.S.A.* **2006**, *103*, 10577.

(17) Beaumont, S. K. *Phys. Chem. Chem. Phys.* **2014**, *16*, 5034.

(18) Iablokov, V.; Beaumont, S. K.; Alayoglu, S.; Pushkarev, V. V.; Specht, C.; Gao, J. H.; Alivisatos, A. P.; Kruse, N.; Somorjai, G. A. *Nano Lett.* **2012**, *12*, 3091.

(19) Saib, A. M.; Moodley, D. J.; Ciobîcă, I. M.; Hauman, M. M.; Sigwebela, B. H.; Weststrate, C. J.; Niemantsverdriet, J. W.; van de Loosdrecht, J. *Catal. Today* **2010**, *154*, 271.

(20) Wang, Z.-J.; Skiles, S.; Yang, F.; Yan, Z.; Goodman, D. W. *Catal. Today* **2012**, *181*, 75.

(21) Saib, A. M.; Borgna, A.; van de Loosdrecht, J.; van Berge, P. J.; Niemantsverdriet, J. W. *J. Phys. Chem. B* **2006**, *110*, 8657.

(22) Lahtinen, J.; Anraku, T.; Somorjai, G. A. *Catal. Lett.* **1994**, *25*, 241.

(23) Schweicher, J.; Bundhoo, A.; Kruse, N. *J. Am. Chem. Soc.* **2012**, *134*, 16135.

(24) Gallas, J. P.; Lavalley, J. C.; Burneau, A.; Barres, O. *Langmuir* **1991**, *7*, 1235.

(25) Papaefthimiou, V.; Dintzer, T.; Dupuis, V.; Tamion, A.; Tournus, F.; Hillion, A.; Teschner, D.; Havecker, M.; Knop-Gericke, A.; Schlogl, R.; Zafeiratos, S. *ACS Nano* **2011**, *5*, 2182.